Available online at www.sciencedirect.com
ScienceDirect
Journal of the European Ceramic Society 30 (2010) 1043–1047
www.elsevier.com/locate/jeurceramsoc

Pulsed electric current, in situ synthesis and sintering of textured TiB_2 ceramics

Songlin Ran, Li Zhang, Omer Van der Biest, Jef Vleugels *

Department of Metallurgy and Materials Engineering (MTM), K.U. Leuven, Kasteelpark Arenberg 44 - bus 2450, B-3001 Heverlee, Belgium

Received 12 June 2009; received in revised form 10 September 2009; accepted 28 September 2009
Available online 23 October 2009

Abstract

Textured TiB_2 monolithic ceramics were prepared in a one step in situ synthesis and densification process during pulsed electric current sintering (PECS) using TiH_2 and amorphous B as raw materials. The Lotgering orientation factors of the (0 0 *l*) and (*h k* 0) planes were measured to be 0.66 and 0.68, respectively. The crystallographically textured ceramics also display a clear microstructural anisotropy. The addition of SiC as a secondary phase was found to deteriorate the orientation in the TiB_2 ceramic due to grain growth inhibition.

Keywords: Titanium diboride; In situ synthesis; Pulsed electric current sintering; Texture; Anisotropy

1. Introduction

In the last few decades, transition metal diborides (TiB_2, ZrB_2, HfB_2, etc.) have become of high research interest as structural ceramics due to their unique combination of physical and chemical properties, including high melting point, high-temperature ablation resistance, good chemical inertness, high thermal and electrical conductivities and high thermal shock resistance.[1,2] ZrB_2 and HfB_2 based ceramics are thought to be the most attractive candidates for ultra-high-temperature ceramics (UHTCs) to be applied in hypersonic flight vehicles, propulsion system, furnace elements, refractory crucibles and high-temperature electrodes.[1] TiB_2 however is more widely used as impact resistant armour, cutting tool, electrode material, crucible and wear resistant coating.[3]

The properties of a ceramic are strongly related to the microstructure. Different methods have been developed to tailor them. Among these methods, texture offers a unique way to improve strength,[4] toughness[5] and wear resistance.[6] Amongst the processes used to induce texture are templated grain growth, hot forging, tape casting, extrusion and the application of a strong magnetic field.[7–11]

Research on textured ceramics mostly focussed on Al_2O_3, Si_3N_4, Sialon and perovskite structure ceramics, but there are only few reports on textured UHTCs. Recently, Ni et al.[12,13] prepared *c*-axis oriented ZrB_2 and HfB_2 based UHTCs by slip casting in a strong magnetic field in combination with SPS. The oxidation resistance was found to be better in the [0 0 1] direction.[12,13]

Preferential TiB_2 grain growth was reported during hot pressing but a combined crystallographic texture and pronounced grain morphology, i.e. aspect ratio of the grains, was not observed.[14] In situ PECS synthesised TiB_2 crystallites, grown from milled Ti and amorphous B starting powders, were claimed to preferably orient with the [0 0 1] orientation parallel to the direction of the applied pressure and DC current.[15] The obtained borides had no pronounced microstructural anisotropy and the microstructure was dominated by needle-shaped crystallites with an inhomogeneous aspect ratio.[15]

In this study, the preparation of textured TiB_2 ceramics by in situ synthesis and consecutive densification in the same die setup during PECS is assessed. The influence of the addition of SiC as a secondary phase on texture formation is also investigated.

2. Experimental procedure

Commercially available TiH_2 (Grade VM, Chemetall, Germany, BET = 2.0 m^2/g), amorphous B (Grade I, H.C. Starck,

* Corresponding author. Tel.: +32 16 321244.
E-mail address: Jozef.Vleugels@mtm.kuleuven.be (J. Vleugels).

0955-2219/$ – see front matter © 2009 Elsevier Ltd. All rights reserved.
doi:10.1016/j.jeurceramsoc.2009.09.030

Germany, BET = 14.7 m^2/g) and SiC (β-SiC, Kaier Nanometer Technology Development Co. Ltd., China, BET = 70 m^2/g) powders were used as starting materials. Monolithic TiB_2 and TiB_2–30 vol.% SiC composites were prepared. The powders were stoichiometrically (TiH_2:B = 1:2) mixed using WC-Co (grade MG15, Ceratizit, Luxembourg) balls in ethanol in a polyethylene container. The mixtures were ball milled for 24 h on a multidirectional mixer (type T2A, WAB, Basel, Switzerland). The slurry was dried at 60 °C in a rotary evaporator. The dried and sieved (325 mesh) powder mixture was loaded into a graphite die/punch setup (Φ = 30 mm) lined with graphite paper. Details on the die/punch/powder assembly is provided elsewhere.[16] The synthesis and densification were conducted by PECS (Type HP D25/1, FCT Systeme, Rauenstein, Germany) in a dynamic vacuum. The TiB_2 monoliths and TiB_2–SiC composites were densified during 3 min at 1800 °C under a pressure of 50 MPa. The temperature was measured axially through the punch by an optical pyrometer, focused on the bottom of the upper punch about 2 mm from the top surface of the sample.

The reaction between TiH_2 and B is highly exothermic. When the heating rate is above a critical value, self-propagating high-temperature synthesis will be initiated, resulting in a sharply increased temperature and excessive H_2 gas release from the TiH_2 phase and high risk of die fracture. According to DSC–TGA measurements on the TiH_2 and B powder mixture, there is an endothermic peak at 516 °C, corresponding to the decomposition of TiH_2. For the sake of protecting the die/punch setup, the heating rate below 900 °C was limited to 10 °C/min.

The crystalline phases and crystallographic orientation were determined by X-ray diffraction (XRD, 3003 TT, Seifert, Ahrensburg, Germany) using Cu Kα radiation with a scanning rate of 0.5°/min. The microstructures of the polished surfaces of the sintered ceramics were examined by scanning electron microscopy (SEM, XL30-FEG, FEI, Eindhoven, Netherlands).

3. Results and discussion

During PECS, the graphite paper on the surface of the TiB_2 monolithic ceramic acts as carbon source resulting in the formation of a small amount of TiC on the sample surface. The XRD pattern of the sandblasted surface, shown in Fig. 1(a), reveals the presence of TiC in addition to TiB_2. No TiC was observed after removal of the surface layer (<0.3 mm) by grinding. According to JCPDS card 35-0741, also indicated on Fig. 1, the intensity of the 1 0 0 diffraction peak of pure TiB_2 is stronger than for 0 0 1. In Fig. 1(a) however, the 0 0 1 intensity is slightly stronger than for the 1 0 0 reflection, indicating textured TiB_2. The XRD patterns of a top surface "TS" and side surface "SS", respectively perpendicular and parallel to the pressing as well as the current flow direction, are compared in Fig. 1.

It is obvious from Fig. 1(b) that the (0 0 1) plane has the strongest relative intensity on the TS surface, whereas the (1 0 0) plane is the most intense on the SS surface (Fig. 1(c)). Because (0 0 l) planes are perpendicular to (h k 0) planes, there is nearly no trace of 1 0 0, 2 0 0 and 1 1 0 peaks on the TS surface. For the same reason, it is difficult to find 0 0 1 and 0 0 2 peaks on the SS surface. The 1 0 1 reflection has a relatively high intensity on both surfaces, as also reported for textured ZrB_2 based ceramics.[2] Since TiB_2 and ZrB_2 are both hexagonal, it can be explained accordingly. First, the (1 0 1) plane intersects (0 0 1) and (1 0 0) planes. Secondly, the average atomic density on the (1 0 1) plane is the highest of all planes. The relative intensity in the XRD pattern increases with the average atomic number of the plane, what is illustrated by the JCPDS 35-0741 reference pattern. Therefore, the presence of 1 0 1 peaks on both surfaces is attributed to the intrinsic crystallographic structure of TiB_2.[12]

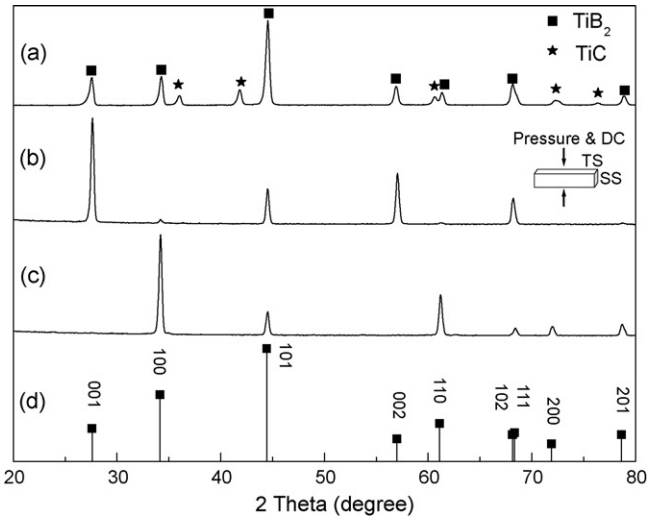

Fig. 1. XRD patterns of the sandblasted TiB_2 surface (a), ground surface perpendicular (b) and parallel (c) to the pressing direction, and JCPDS card 35-0741 (d).

The crystallographic difference between the TS and SS surfaces can be quantified by comparing the $I_{(0\,0\,l)}/I_{(1\,0\,1)}$ and $I_{(h\,k\,0)}/I_{(1\,0\,1)}$ intensity ratios. As summarised in Table 1, the $I_{(0\,0\,l)}/I_{(1\,0\,1)}$ ratio on the TS surface was substantially higher than on the SS surface, whereas the $I_{(h\,k\,0)}/I_{(1\,0\,1)}$ ratio shows the opposite trend. After in situ synthesis and densification, the c-axis of the TiB_2 grains shows a preferred orientation perpendicular to the top surface. The degree of texture formation is evaluated by the Lotgering orientation factor, f, defined by the following equations:[17]

$$f = \frac{p - p_0}{1 - p_0}, \quad p_0 \text{ and } p = \frac{\sum I_{h'\,k'\,l'}}{\sum I_{h\,k\,l}} \tag{1}$$

with $\sum I_{(h'\,k'\,l')}$ and $\sum I_{(h\,k\,l)}$ the integrated intensities of the $h'\,k'\,l'$ and $h\,k\,l$ reflections. p_0 and p represent a random oriented and a ($h'\,k'\,l'$) textured material, respectively. In this study, the p and p_0 values were calculated according to the data obtained from XRD patterns and JCPDS card 35-0741, respectively.

Table 1
XRD peak intensity ratios.

	JCPDS 35-0471	TS surface	SS surface
$I_{(0\,0\,l)}/I_{(1\,0\,1)}$	0.34	4.35	0
$I_{(h\,k\,0)}/I_{(1\,0\,1)}$	0.89	0.13	6.45

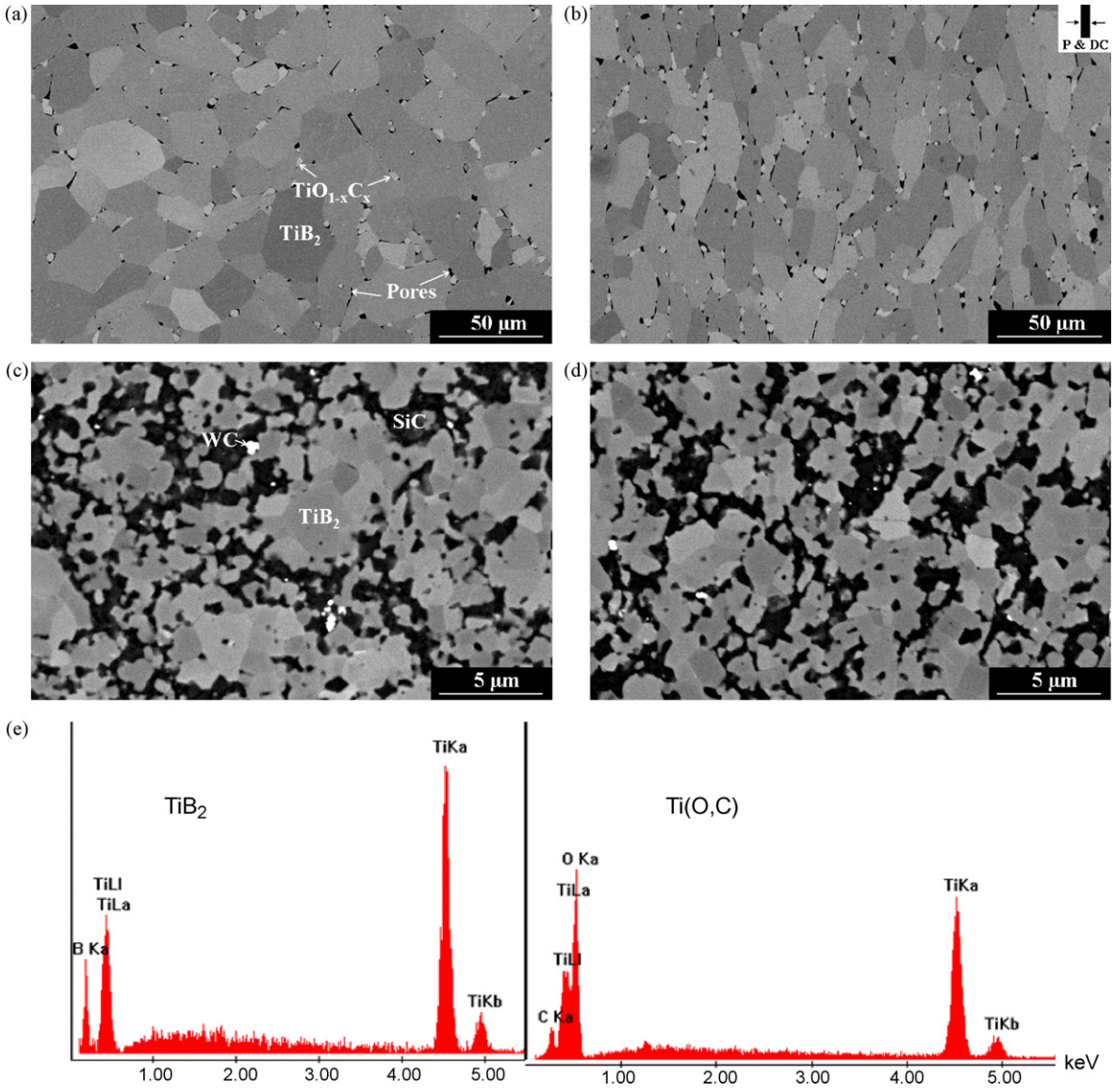

Fig. 2. Backscattered electron micrographs of polished TS (a and c) and SS (b and d) surfaces of TiB_2 (a and b) and TiB_2–30 vol.% SiC (c and d), and EDS point analyses (e) of the phases in (a) and (b).

The Lotgering orientation factor of the (0 0 *l*) and (*h k* 0) planes ranges from 0 for a randomly oriented material to 1 for a fully textured material, and was measured to be 0.66 and 0.68 respectively for the PECS TiB_2.

Highly textured ZrB_2 and HfB_2 based ceramics with Lotgering orientation factors of the (0 0 1) plane above 0.90, prepared by means of slip casting in a 12 T magnetic field and subsequent densification by pulsed electric current sintering, were recently reported.[12,13] Microstructural analysis however did not reveal any morphological difference between the surfaces perpendicular and parallel to the pressing direction.[12,13] It is well known that elongated grains can act as reinforcements to improve mechanical properties such as flexure strength and fracture toughness.[18,19] Hexagonal cross-sections as well as elongated TiB_2 grains were simultaneously observed on cross-sectioned PECS TiB_2/Cu cermets.[20]

In the present work, the textured TiB_2 also has a clear microstructural anisotropy, as shown in Fig. 2(a) and (b), with the *a*- and *b*-axis of the elongated TiB_2 grains aligned perpendicular to the pressure and current (P and DC) direction. The TiB_2 grains have a clear hexagonal platelet shape with a thickness of 10.12 ± 2.18 μm and a diameter of 21.60 ± 6.21 μm, as measured by the linear intercept method of 50 grains. In both Fig. 2(a) and (b), a secondary phase was found at the triple junctions and along some grain boundaries. EDS point analysis of the constituent phases (see Fig. 2(e)) indicated that the bulk phase is TiB_2 whereas the smaller grains contain Ti, O and C. This secondary phase was assumed to be $TiO_{1-x}C_x$ which was also reported to be present in hot pressed TiB_2.[21] Volatile boron oxide was claimed to be reduced by graphite surrounding the sample to produce CO gas, which transported carbon into the densifying powder compact to form $TiO_{1-x}C_x$.[21] The titanium

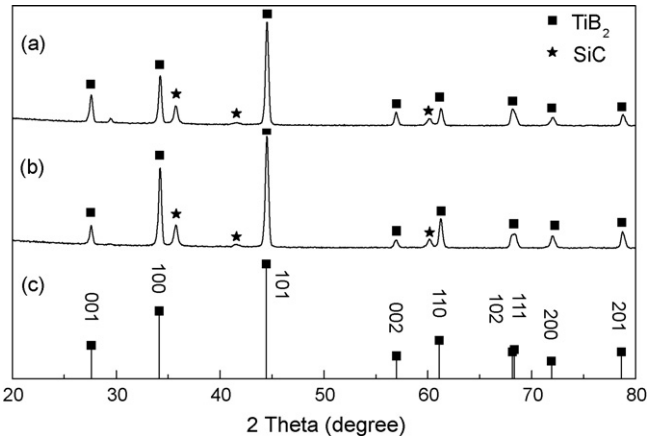

Fig. 3. XRD patterns of ground TS (a) and SS (b) surfaces of TiB_2–30 vol.% SiC together with JCPDS card 35-0741 (c).

oxide and boron oxide were present on the surface of the ZrH_2 and B starting powders, whereas the carbon interdiffused from the graphite die and punches. The traces of bright atomic number contrast WC, clearly visible in Fig. 2(c) and (d), originated from the WC-Co milling medium used. Both $TiO_{1-x}C_x$ and WC were not detected by XRD due to their low content.

The density of the ground TiB_2 ceramic was measured to be 4.45 g/cm^3. Assuming a theoretical density of 4.52 g/cm^3 would imply a residual porosity of about 1.5 vol.%. It is worthwhile noting that nearly all the pores are located at the grain boundaries and no pores are present inside the TiB_2 grains. Baik et al. investigated the effect of oxygen contamination on the densification of TiB_2, revealing that most pores were inside the grains for high-oxygen content TiB_2 grades whereas mainly intergranular pores were observed for low-oxygen ceramics.[22] Oxygen enhanced grain boundary diffusion and promoted the grain coarsening by accelerating evaporation and condensation kinetics.[22] In this work, the TiB_2 was in situ synthesized from TiH_2, allowing to limit the oxygen contamination to a minimum. The low-oxygen content is in agreement with the intergranular residual porosity.

The formation of textured TiB_2 is attributed to preferential orientation growth of the TiB_2 grains. When hot pressing commercial micrometer sized TiB_2 powders, grains tended to grow with the [0 0 1] zone axis parallel to the applied pressure direction.[14] During PECS, the interaction of the magnetic field induced by the DC current was also thought to assist to orient TiB_2 crystallites.[15]

Comparing the XRD spectra of the sandblasted and ground TS surfaces in Fig. 1 suggests that the presence of the secondary TiC phase largely deteriorates the orientation of TiB_2. To prove this, TiB_2 composites with 30 vol.% SiC grain growth inhibitor were prepared according to the same processing route using TiH_2, amorphous B and SiC starting powders. XRD (Fig. 3) and SEM (Fig. 2) results indicated that there was no clear difference between TS surface and SS surface. The calculated Lotgering orientation factors of (0 0 l) and (h k 0) were only 0.05 and 0.13, suggesting a random TiB_2 grain orientation. In contrast however, the orientation of HfB_2 grains prepared by slip casting in a strong magnetic field alignment was reported to slightly increase with the addition of SiC.[13] Obviously, the orientation mechanism in this case is different since crystallographic orientation is due to the anisotropic magnetic susceptibility of the diboride and the secondary SiC phase has no adverse effect. In the case of in situ synthesis and sintering, TiB_2 grains grow with a preferred orientation and limiting the TiB_2 grain growth by grain boundary pinning clearly inhibits microstructural and crystallographic texture development. The grain size of TiB_2 decreased to ~2 μm when adding 30 vol.% SiC.

4. Conclusions

Microstructurally as well as crystallographically textured monolithic TiB_2 was prepared by in situ synthesis during pulsed electric current sintering for 3 min at 1800 °C and 50 MPa from TiH_2 and amorphous B. The Lotgering orientation factors of the (0 0 l) and (h k 0) planes were 0.66 and 0.68, respectively. Due to the low-oxygen content in the material, the residual porosity (~1.5 vol.%) was located at the grain boundaries. Texture formation was attributed to the preferred TiB_2 grain growth in the direction perpendicular to the applied pressure, since texture formation could be inhibited by the addition of a SiC grain growth inhibitor.

Acknowledgements

This work was supported by the Research Fund of K.U. Leuven under project GOA/08/007 and the Flanders-China bilateral project BIL 07/06.

References

1. Fahrenholtz, W. G., Hilmas, G. E., Talmy, I. G. and Zaykoski, J. A., Refractory diborides of zirconium and hafnium. *J. Am. Ceram. Soc.*, 2007, **90**, 1347–1364.
2. Guo, S. Q., Densification of ZrB_2-based composites and their mechanical and physical properties: a review. *J. Eur. Ceram. Soc.*, 2009, **29**, 995–1011.
3. Munro, R. G., Material properties of titanium diboride. *J. Res. Natl. Inst. Stand. Technol.*, 2000, **105**, 709–720.
4. Hirao, K., Ohashi, M., Brito, M. E. and Kanzaki, S., Processing strategy for producing highly anisotropic silicon nitride. *J. Am. Ceram. Soc.*, 1995, **78**, 1687–1690.
5. Ohji, T., Hirao, K. and Kanzaki, S., Fracture resistance behavior of highly anisotropic silicon nitride. *J. Am. Ceram. Soc.*, 1995, **78**, 3125–3128.
6. Nakamura, M., Yamauchi, Y. and Kanzaki, S., Tribological properties of unidirectionally aligned silicon nitride. *J. Am. Ceram. Soc.*, 2001, **84**, 2579–2584.
7. Wei, M., Zhi, D. and Brandon, D. G., Microstructure and texture evolution in gel-cast α-alumina/alumina platelet ceramic composites. *Scr. Mater.*, 2005, **53**, 1327–1332.
8. Zhu, X., Suzuki, T. S., Uchikoshi, T. and Sakka, Y., Highly texturing β-Sialon via strong magnetic field alignment. *J. Am. Ceram. Soc.*, 2008, **91**, 620–623.
9. Gelfuso, M. V., Thomazini, D. and Eiras, J., Synthesis and structural, ferroelectric, and piezoelectric properties of $SrBi_4Ti_4O_{15}$ ceramics. *J. Am. Ceram. Soc.*, 1999, **82**, 2368–2372.
10. Watanabe, H., Kimura, T. and Yamaguchi, T., Particle orientation during tape casting in the fabrication of grain-oriented bismuth titanate. *J. Am. Ceram. Soc.*, 1989, **72**, 289–293.
11. Takeuchi, T., Tani, T. and Saito, Y., Unidirectionally textured $CaBi_4Ti_4O_{15}$ ceramics by the reactive templated grain growth with an extrusion. *Jpn. J. Appl. Phys.*, 2000, **39**, 5577–5580.

12. Ni, D.-W., Zhang, G.-J., Kan, Y.-M. and Sakka, Y., Highly textured ZrB_2-based ultrahigh temperature ceramics via strong magnetic field alignment. *Scr. Mater.*, 2009, **60**, 615–618.
13. Ni, D.-W., Zhang, G.-J., Kan, Y.-M. and Sakka, Y., Textured HfB_2-based ultrahigh-temperature ceramics with anisotropic oxidation behavior. *Scr. Mater.*, 2009, **60**, 913–916.
14. Jensen, M. S., Einarsrud, M.-A. and Grande, T., Preferential grain orientation in hot pressed TiB_2. *J. Am. Ceram. Soc.*, 2007, **90**, 1339–1341.
15. Schmidt, J., Boehling, M., Burkhardt, U. and Grin, Y., Preparation of titanium diboride TiB_2 by spark plasma sintering at slow heating rate. *Sci Technol. Adv. Mater.*, 2007, **8**, 376–382.
16. Vanmeensel, K., Laptev, A., Hennicke, J., Vleugels, J. and Van der Biest, O., Modelling of the temperature distribution during field assisted sintering. *Acta Mater.*, 2005, **53**, 4379–4388.
17. Lotgering, F. K., Topotactical reactions with ferrimagnetic oxides having hexagonal crystal structures-I. *J. Inorg. Nucl. Chem.*, 1959, **9**, 113–123.
18. Imamura, H., Brito, M. E., Toriyama, M. and Kanzaki, S., Further improvement in mechanical properties of highly anisotropic silicon nitride ceramics. *J. Am. Ceram. Soc.*, 2000, **83**, 495–500.
19. Zenotchkine, M., Schuba, R., Kim, J.-S. and Chen, I.-W., Effect of seeding on the microstructure and mechanical properties of α-SiAlON. I. γ-SiAlON. *J. Am. Ceram. Soc.*, 2002, **85**, 1254–1259.
20. Venkateswaran, T., Basu, B., Raju, G. B. and Kim, D. Y., Densification and properties of transition metal borides-based cermets via spark plasma sintering. *J. Eur. Ceram. Soc.*, 2006, **26**, 2431–2440.
21. Jensen, M. S., Einarsrud, M.-A. and Grande, T., The effect of surface oxides during hot pressing of TiB_2. *J. Am. Ceram. Soc.*, 2009, **92**, 623–630.
22. Baik, S. and Becher, P. F., Effect of oxygen contamination on densification of TiB_2. *J. Am. Ceram. Soc.*, 1987, **70**, 527–530.